Mode-locking of acoustic resonators and its application to vibration cancellation in acoustic heat engines

P. S. Spoor and G. W. Swift
Condensed Matter and Thermal Physics Group, Los Alamos National Laboratory, Los Alamos, New Mexico 87545

(Received 10 February 1999; accepted for publication 10 June 1999)

Vibration induced in engine hardware by a working fluid can be very significant in high-power, high-amplitude acoustic heat engines, and is a serious impediment to their practical use. This vibration can cause fatigue and destruction of engine components as well as fuel lines, cooling lines, and sensor wires. The forces involved make anchoring such an engine to an ''immovable'' object impractical. Rigidly attaching two such engines together, and acoustically coupling them with a duct of such a length and diameter that the two engines mode-lock in antiphase (thus canceling the longitudinal vibration) appears to be an inexpensive, viable solution. This paper describes in detail experiments demonstrating the feasibility of this idea, and the underlying theory. © *1999 Acoustical Society of America.* [S0001-4966(99)03909-0]

PACS numbers: 43.35.Ud [HEB]

INTRODUCTION

In recent years, considerable progress has been made in designing practical heat engines that have no moving parts, other than acoustic oscillations in the working fluid;[1] such engines work on principles loosely exemplified by such devices as the Sondhauss tube[2,3] and the Rijke tube,[4] where heat suitably applied to a tube causes spontaneous oscillation of the gas inside. Thermoacoustic heat engines have the advantage of no bearings or sliding seals, so they hold out the possibility of extreme simplicity and reliability. In order to achieve useful power densities, however, the engines must contain a working fluid under high pressure, oscillating with an amplitude on order of 10% or more of mean pressure. Thus the working fluid is capable of exerting enormous oscillating force on the structure surrounding it, inducing intense vibration in the engine hardware. Far from being a mere nuisance, this vibration can be downright terrifying in an engine of appreciable size; a one-ton prototype that produces 20 kW of acoustic power[5] experiences several g's of acceleration when operating full tilt.

The need to control this vibration has been understood from the earliest days of thermoacoustic research; in a 1958 patent detailing heat-driven acoustic devices, Marrison[6] describes two heat-driven acoustic resonators, intended to drive small linear alternators, joined end-to-end as shown in Fig. 1, to achieve vibration cancellation. The original patent reads:

> ...a pair of devices...juxtaposed in end-to-end relation for dynamic balance. In order that there shall be adequate coupling between the two vibrating gas columns, a channel is provided that interconnects them...In the operation of this balanced arrangement, the movement of the gas at any instant is either inward toward the central plane of both cylinders, or outward toward the separated ends of the two cylinders. Thus the vibration of each gas column finds a reaction in the vibration of the other gas column so that dynamic balance is secured, and external vibration, shaking of the mount, noise, and the like are minimized.

The interconnecting channel is necessary because thermoacoustic engines, like organ pipes or pendulum clocks, are self-maintained oscillators, and a pair will not naturally run at the same frequency, or in a particular phase relationship, unless they are coupled sufficiently.

The mode-locking of coupled, self-maintained oscillators was first described by Christiaan Huygens in 1665, who reported in a letter to his father[7] that a pair of large pendulum clocks sitting a few feet apart would synchronize their ticks; he further noted that

> If two rhythms are nearly the same and their sources are in close proximity, they will always lock up, fall into synchrony, entrain.

Following Huygens, we suppose that if two acoustic engines are nearly the same in natural frequency and coupled in some way with sufficient strength, they may entrain, thus locking to each other in frequency and phase. This principle is implicit in the Marrison device, and in this work we explicitly aim for an understanding of it, so it may be used to the greatest advantage in minimizing vibration.

Marrison's concept requires the tandem system of two engines to be twice as long as a single engine. Acoustic engines, requiring as they do a resonator which is a significant fraction of a wavelength (usually a half wavelength), tend to be large already, and a vibration-cancellation method that does not require additional length is clearly preferable. We instead consider two engines mounted side-by-side rather than end-to-end, with two neighboring ends connected by a narrow, bent duct a half-wavelength long. The acoustic pressure at the neighboring ends will tend to be in antiphase, thus encouraging the movement of the gas in each engine to be opposite the movement in the other. We show that mode-locking and vibration cancellation in such an arrangement can be achieved by careful consideration of how the locked state depends on engine and coupler geometry, the working

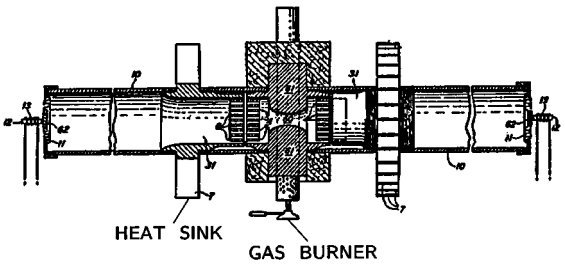

FIG. 1. W. A. Marrison's original concept, from a 1958 patent, for two acoustic engines mounted in opposition for dynamic balance, with a narrow channel coupling the two (Ref. 6).

fluid properties, and the difference in natural frequencies of the two engines.

Our experiments use two small (acoustic power$\approx$5 W, length$=$1.75 m, diameter$=$35 mm) thermoacoustic engines whose cases are welded together. They are coupled acoustically by one of a number of ducts nominally half a wavelength long, with radii ranging from 1/14th to 1/7th of the engine resonator radius. The working fluid for most of the measurements is air at 80 kPa, which is atmospheric pressure in Los Alamos, elevation 2200 m. Mode-locking of the engines, with their acoustic oscillations in antiphase, is readily achieved; measurements of frequency, pressure amplitude, and phase, as well as accelerometer measurements on the cases, indicate that 90% of the case vibration is canceled by using a coupler which is 3.5 mm in diameter, or one-tenth of the diameter of an engine resonator, if the engines are not more than 0.2% apart in natural (uncoupled) frequency. The sensitivity to frequency difference is partly a consequence of our system's small size; numerical simulations indicate that for a 30-bar He system whose engine resonators are 10 times the diameter of those in our small test system, a coupler one-tenth the engine resonator diameter allows cancellation of 95% percent of case vibration, when the engines' natural frequencies are as much as 1% different. This simulation, applicable to the 20-kW engine mentioned earlier, implies that our method should prove useful.

In addition to the measurements and simulations mentioned above, we have developed a simple theory to explain the dependence of the phase of the locked state (and hence the degree of vibration cancellation) on the coupler dimensions, fluid properties, and the difference in the engines' natural frequencies. We find that theory, simulation, and experiment all agree extremely well for our small test system, which provides encouragement that our methods can be relied upon to help design larger and more complex mode-locked acoustic systems.

Our engines can also mode-lock by ''mass coupling'' through their shared structure, with no acoustic coupling at all. This effect, which will be detailed in a separate paper,[8] is too weak to be a major concern in the vibration cancellation problem.[9]

I. THEORY

An excellent introduction to mode-locking can be found in Chapter 12 of A. B. Pippard's impressive book, *The Physics of Vibration*,[10] and we shall draw extensively from his work in developing our own theoretical model. Pippard considers the mode-locking of discrete systems such as LRC circuits; one of the interesting aspects of the present work is that acoustic systems contain the additional complexity of spatial dimension. Therefore we review some properties of passive, coupled acoustic resonators before considering the full mode-locking problem.

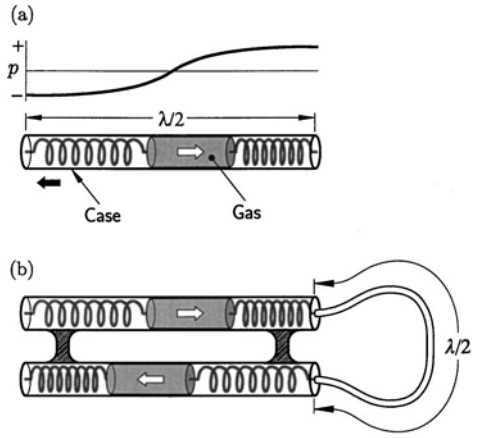

FIG. 2. Mass-and-spring models of half-wavelength acoustic resonators, showing (a) a single resonator, with a plug of gas bouncing off gas springs on the ends, and (b) two such resonators, rigidly attached, and coupled by a narrow half-wavelength duct to invert the phase of the pressure, thus encouraging the two resonators to oscillate in antiphase. Here λ stands for wavelength.

A. Coupled passive half-wave acoustic resonators

Figure 2 illustrates the basic case-vibration problem and our proposed solution. In Fig. 2(a), a single resonator's case moves in response to the motion of the gas inside; the frequency is such that the resonator's length is λ/2, where λ is the wavelength. This case motion can be analyzed either in terms of the axial forces exerted on its ends by the oscillating pressures inside, or in terms of momentum conservation, which requires that the case momentum be equal in magnitude but opposite in direction to the gas momentum at any instant. In Fig. 2(b) a half-wavelength coupler has been added to invert the pressure between two rigidly attached resonators, so that the acoustic oscillations are in antiphase and the net axial force exerted by the oscillating gas on the assembly is zero. In order to achieve such vibration suppression, the system of three coupled ducts must favor a normal mode corresponding to a half-wavelength in each duct, with the two large ducts (the resonators) oscillating in antiphase. Let the radius of the resonators be r_0 and the radius of the coupler be r_c; in the approximation that the ducts are all lossless and have the same length l, and $r_0 \gg r_c$, the normal mode frequencies in the neighborhood of $f=a/2l$ are easily obtained:

$$f_0 = \frac{a}{2l} \tag{1}$$

and

$$f_\pm \approx \frac{a}{2l}\left(1 \pm \frac{\sqrt{2}}{\pi}\frac{r_c}{r_0}\right), \tag{2}$$

where a is the sound speed. One solution, f_0, is the same as for a single duct, and corresponds to exactly a half-wavelength in each duct, with pressure nodes in the center of each duct, and velocity nodes at the two rigid ends and at each of the two junctions. Since velocity is zero at these junctions, matching volume velocities on either side does not require a discontinuity in velocity; hence, the coupler has the same waveshape and magnitude of oscillation as the resonators do. This is the desired antiphase mode, where the pressure oscillations in the resonators are π out of phase.

By contrast, f_+ and f_- correspond to ''in-phase'' modes, which tend to maximize case vibration rather than eliminate it. However, these modes have nonzero velocity at the junctions, and so the amplitude of oscillation in the coupler is much larger than that in the resonators. Although this analysis is based on lossless acoustics, the large oscillation amplitude in the coupler suggests that these in-phase modes are much lossier than the antiphase mode, so the antiphase mode is more likely to be selected. In fact, we have never observed anything but the antiphase mode in our mode-locked engines. In the antiphase mode the resonators and the coupler have the same oscillating pressure and velocity amplitudes, so the ratio of coupler to resonator dissipation in the thermoviscous boundary layer near the wall is simply the ratio of their radii. If this behavior is a good approximation for what actually happens when two acoustic engines are coupled together, a narrow coupler is less lossy than a wide one. Thus if resonator losses are significant in an engine, there is motivation for keeping the connecting duct narrow when coupling two together, to minimize additional loss.

B. Coupled, maintained acoustic resonators

The discussion of coupled duct resonators at the beginning of this section treated the two resonators and coupler as one composite resonator, with well-defined normal modes. A system of two self-maintained oscillators coupled with a narrow duct actually has a much richer behavior, such as that observed by supplying two similar organ flue pipes or slide whistles with compressed air so that they sound stable tones, and allowing them to couple by bringing their mouths in close proximity. When the pipes are far apart, they ''sing'' with their separate natural frequencies; one hears a ''beating'' at the difference frequency. As the pipes are brought closer together, this beat frequency slows, and then abruptly stops—at which point the pipes are locked in frequency and phase. The frequency of an individual pipe is sensitive to conditions at the mouth of the pipe; when the two pipes are close enough to interact, they may alter each other's frequencies enough to eventually phase lock, if their natural frequencies are not too different. Our coupled thermoacoustic engines display roughly the same behavior as these coupled organ pipes, and we will let our analytic approach be guided by this concept of beating slowed or stopped by coupling.

Before proceeding with our theory, it will be helpful to define exactly what information we seek. Mode-locking in acoustic oscillators is a broad enough subject that we cannot present an exhaustive treatment here. Rather, we will limit our inquiry at the outset to those aspects that we expect will be most relevant to the vibration-cancellation problem.

One important difference between coupled passive oscillators and coupled maintained oscillators is that in the passive system, the vibrations of the individual oscillators are either exactly in phase with each other or exactly antiphase. When the oscillators are maintained, however, this is no longer true, and a weakly coupled pair of very closely matched maintained oscillators may lock with essentially arbitrary phase. In addition, the amplitudes in each oscillator may be substantially different (true of a passive system as well, if the coupling is sufficiently weak). This may be seen quite readily in the organ pipe demonstration described above, if pressure sensors are placed in each pipe.

This has important consequences for us—for maximum vibration cancellation, our coupled resonators must be in antiphase *and* the amplitudes in both sides must be matched. If we let

$$\begin{aligned} \phi &= \text{phase difference between the resonators} \\ \zeta &= \text{ratio of pressure amplitudes in the resonators,} \end{aligned} \tag{3}$$

and consider the axial forces exerted by the oscillating fluid on the structure of our coupled system, we can express the degree of vibration cancellation in terms of ϕ and ζ. If we define a vibration-cancellation ratio

$$R_V = 1 - \frac{\text{amplitude of case vibration (coupled engines)}}{\text{amplitude of case vibration (one engine alone)}}, \tag{4}$$

then it is found that

$$R_V = 1 - [(1+\zeta\cos\phi)^2 + \zeta^2 \sin^2\phi]^{1/2}, \tag{5}$$

or

$$R_V \approx 1 - [(\zeta-1)^2 + (\phi-\pi)^2]^{1/2}, \quad \text{if} \quad \zeta \approx 1, \quad \phi \approx \pi. \tag{6}$$

Thus the quantities of most interest to us are ϕ and ζ; in particular, we seek their sensitivities $\partial\phi/\partial\Delta\omega$ and $\partial\zeta/\partial\Delta\omega$ to the mistuning $\Delta\omega$ of the resonators, $\Delta\omega$ being the difference in the resonators' uncoupled natural frequencies. To further simplify our analysis, we will assume that the coupler itself is in resonance. This seems intuitively like a desirable condition, based on the lossless analysis of Sec. I A and since it would appear to allow the maximum transmission of energy from one resonator to the other. This assumption has another interesting, nonintuitive consequence as well. If we treat the coupler as an impedance coupling two acoustic circuits, the resonant coupler corresponds to a coupling impedance which is all real (resistive). A resistively coupled pair of maintained oscillators has some curious properties;[11] among them is that the amplitude in both oscillators must be identical, regardless of the phase angle! This fortuitous result not only makes our vibration-cancellation job easier, but it greatly simplifies the analysis. It implies that if we assume a resonant coupler and let $\phi \simeq \pi$, we can set $\zeta = 1$ without any loss of information. Thus the extent of vibration cancellation is given by ϕ alone, and its rate of change with $\Delta\omega$ is given by $\partial\phi/\partial\Delta\omega$ alone.

It should be noted that for very narrow couplers, where the thermoviscous boundary layer is an appreciable fraction of the coupler radius, experiments and simulations show that

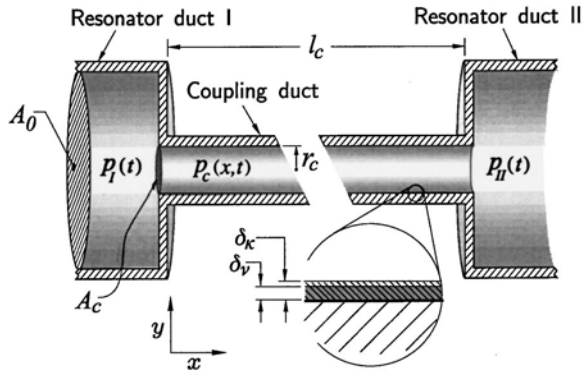

FIG. 3. Details of the junctions between two resonators and the coupling duct that connects them. For vibration cancellation, the system should be ''folded'' as shown in Fig. 2(b).

a coupler shorter than the resonant length provides the optimum vibration cancellation, even though it allows some amplitude imbalance.

Figure 3 shows the details of the interface between the resonators and the coupling duct. The oscillating pressure in resonator I at the junction with the coupler is $p_{\mathrm{I}}(t)$; that in resonator II is $p_{\mathrm{II}}(t)$. We let the end of the coupler at p_{I} be $x=0$, and that at p_{II} be $x=l_c$, where l_c is the length of the coupler. These pressures should be in antiphase in order to cancel vibration in the resonator cases. Note the blowup of the boundary layer near the coupler wall, indicating the viscous and thermal penetration depths δ_ν and δ_κ. We assume the two resonators (and the coupler) contain the same working gas in the same state, and the resonators are identical except for a small difference in natural frequency, due to a slight difference in gas temperature, for instance. Let the natural frequency of resonator I be ω_{I} and that of resonator II be ω_{II}; by ''natural frequency'' we mean the frequency that a resonator would have if it were uncoupled from the other. The mistuning can then be defined as

$$\Delta\omega=\omega_{\mathrm{II}}-\omega_{\mathrm{I}}. \tag{7}$$

We also assume the coupling is weak and perturbs only slightly the uncoupled behavior of each resonator. If the resonators are *not* locked, the oscillations in the resonators are modulated by a relatively slow beat envelope, like the organ pipes previously discussed, and the beating is slowed and eventually stopped by increasing the coupling. Thus we can write:

$$p_{\mathrm{I}}(t)=\Re\{P_{\mathrm{I}}(t)e^{i[\omega t+\phi_{\mathrm{I}}(t)]}\}, \tag{8}$$

$$p_{\mathrm{II}}(t)=\Re\{P_{\mathrm{II}}(t)e^{i[\omega t+\phi_{\mathrm{II}}(t)]}\}, \tag{9}$$

where $\Re\{\}$ indicates taking the real part. We assume $P_{\mathrm{I,II}}$ and $\phi_{\mathrm{I,II}}$ are real and slowly varying compared to ω, and $P_{\mathrm{I,II}}$ are always $\geqslant 0$. The relative phase ϕ and amplitude ratio ζ introduced in Eq. (3) may now be defined as:

$$\phi=\phi_{\mathrm{II}}-\phi_{\mathrm{I}}, \qquad \zeta=\frac{P_{\mathrm{II}}}{P_{\mathrm{I}}}. \tag{10}$$

We let the compromise frequency ω be a constant; the apparent *instantaneous* difference in frequency between resonators I and II is simply $\Delta\omega_{\mathrm{inst.}}=\partial\phi/\partial t$.

To obtain a pair of coupled differential equations, we start with a homogeneous equation for one of the maintained resonators, which it obeys when uncoupled:

$$\frac{d^2p_{\mathrm{I}}}{dt^2}+\omega_{\mathrm{I}}^2p_{\mathrm{I}}+\frac{\omega_{\mathrm{I}}}{Q}\left(1-\frac{P_0^n}{P_{\mathrm{I}}^n}\right)\frac{dp_I}{dt}=0. \tag{11}$$

The feedback that maintains the oscillations at or near frequency ω_{I} and amplitude P_0 is provided by the term $(\omega_{\mathrm{I}}/Q)(1-P_0^n/P_{\mathrm{I}}^n)dp_{\mathrm{I}}/dt$; this causes the amplitude to relax toward P_0 should the amplitude be initially higher or lower than P_0. This type of equation is found in Pippard[12] and in Van der Pol's paper on maintained triode oscillators.[13] The quantity Q is more or less the passive quality factor of the oscillator; this and the exponent n determine the relaxation time. For this work, the value of n is not important;[14] for further discussion, see Ref. 8. For convenience, we choose $n=2$.

Let $u_c(x,t)$ denote the x-component of particle velocity in the coupler, spatially averaged over the coupler cross-section. If, due to coupling, a volume velocity $-A_cu_c(0,t)$ enters the resonator from the coupler, the resonator obeys the inhomogeneous equation[15,16]

$$\frac{d^2p_{\mathrm{I}}}{dt^2}+\omega_{\mathrm{I}}^2p_{\mathrm{I}}+\frac{\omega_{\mathrm{I}}}{Q}\left(1-\frac{P_0^2}{P_{\mathrm{I}}^2}\right)\frac{dp_{\mathrm{I}}}{dt}=-\frac{2\rho a^2}{l_0}\left(\frac{A_c}{A_0}\right)\frac{du_c(0,t)}{dt}. \tag{12}$$

(The ''source term'' on the right-hand side has a minus sign because we define x and u_c positive pointing into the coupler from the resonator.) Here l_0 is the length of a resonator, A_0 is its cross-sectional area, A_c is the area of the coupler, ρ is the (average) density, and a is the (average) sound speed. A similar equation can be constructed for p_{II}. To couple the equations to one another, we solve for the complex particle velocity in the coupler $u_c(x,t)=\Re\{\tilde{u}_c(x)e^{i\omega t}\}$ (where $\sim$ indicates a complex quantity), subject to the boundary conditions $\tilde{p}_c(0)=P_{\mathrm{I}}e^{i\phi_{\mathrm{I}}}$ and $\tilde{p}_c(l_c)=P_{\mathrm{II}}e^{i\phi_{\mathrm{II}}}$, to obtain

$$\tilde{u}_c(x)=P_{\mathrm{I}}e^{i\phi_{\mathrm{I}}}\frac{\tilde{k}_c}{i\omega\rho}\left[\sin\tilde{k}_cx+\frac{\cos\tilde{k}_cl_c-\zeta e^{i\phi}}{\sin\tilde{k}_cl_c}\cos\tilde{k}_cx\right]. \tag{13}$$

Because the coupler is assumed lossy, we use a complex wave number $\tilde{k}_c$ which is approximately:

$$\tilde{k}_c\approx\frac{\omega}{a_c}\left[\left(1+\frac{\delta}{2r_c}\right)-\frac{\delta}{2r_c}i\right], \tag{14}$$

where

$$\delta=\delta_\nu+(\gamma-1)\delta_\kappa; \tag{15}$$

r_c is the radius of the coupler, a_c is the bulk speed of sound in the coupler, and δ_ν and δ_κ are the viscous and thermal penetration depths, respectively. Here we are making the simplifying, although not wholly accurate, assumption that $r_c\gg\delta_\kappa$ or δ_ν. Later we discuss how it might affect our results.

At this stage, our analysis has much in common with the work of Pippard[10] and Fletcher.[17] Were we interested in the dynamic behavior of the system as it approaches a locked state, we could continue the analysis by carrying out the time

derivatives in Eq. (12) and in the corresponding equation for $p_{II}(t)$, discarding small terms, and solving for $\partial\phi/\partial t$ and $\partial\zeta/\partial t$. However, we are interested primarily in the locked states, where $\partial\phi/\partial t=0$ and $\partial\zeta/\partial t=0$, so we assume simply that $d/dt=i\omega$. If we also assume that $\zeta=1$, i.e., $P_I=P_{II}=P$ (resonant coupler), the following pair of equations may be obtained:

$$-(\omega^2-\omega_I^2)+i\omega\frac{\omega_I}{Q}\left(1-\frac{P_0^2}{P^2}\right)$$

$$=-\frac{2a^2}{l_0}\left(\frac{A_c}{A_0}\right)\frac{\tilde{k}_c}{\sin\tilde{k}_c l_c}[\cos\tilde{k}_c l_c-e^{i\phi}] \tag{16}$$

and

$$-(\omega^2-\omega_{II}^2)+i\omega\frac{\omega_{II}}{Q}\left(1-\frac{P_0^2}{P^2}\right)$$

$$=-\frac{2a^2}{l_0}\left(\frac{A_c}{A_0}\right)\frac{\tilde{k}_c}{\sin\tilde{k}_c l_c}[\cos\tilde{k}_c l_c-e^{-i\phi}]. \tag{17}$$

Subtracting Eq. (16) from Eq. (17), while noting that $\omega_I\approx\omega_{II}\approx\omega$ and $|1-P_0^2/P^2|\ll 1$, gives

$$-\omega\Delta\omega\approx\frac{a^2}{l_0}\left(\frac{A_c}{A_0}\right)\frac{\tilde{k}_c}{\sin\tilde{k}_c l_c}2i\sin\phi. \tag{18}$$

A resonant coupler implies $\Re\{\tilde{k}_c l_c\}=\pi$; thus we have $\tilde{k}_c\approx\pi/l_c-i(\omega/a_c)(\delta/2r_c)$. With appropriate use of the approximations a_c, a_I, $a_{II}\approx a$, $l_c\approx l_0$, and $\delta/r_c\ll 1$, taking the real part of Eq. (18) and rearranging gives

$$\sin\phi\approx-\frac{\pi^2}{4\omega}\left(\frac{A_0}{A_c}\right)\frac{\delta}{r_c}\Delta\omega. \tag{19}$$

Finally, we let $\phi\simeq\pi$, and differentiate with respect to $\Delta\omega$; the result can be expressed in dimensionless form as:

$$\left(\frac{\omega}{\pi}\right)\frac{\partial\phi}{\partial\Delta\omega}=\frac{\pi}{4}\left(\frac{A_0}{A_c}\right)\frac{\delta}{r_c}. \tag{20}$$

The factor $1/\pi$ on the left-hand side effectively normalizes the phase angle—most mode-locked systems (including our acoustic engines) become unlocked at $\phi=\pm\pi/2$, so the range of ϕ is about π radians.

This equation, although clearly the result of many approximations, has the advantage of being simple to interpret. It tells us how the phase of the locked state changes as a function of the (fractional) mistuning $\Delta\omega/\omega$, the geometry, and the thermoviscous properties of the working fluid. In the present context, this effectively tells us how the degree of vibration cancellation is affected by all these parameters. The factor A_0/A_c is the ratio of resonator to coupler area; the factor r_c/δ is approximately the quality factor Q of the coupler.[18] In general, we want $\partial\phi/\partial\Delta\omega$ to be small—i.e., we want vibration to increase only slightly as our engines become more mistuned; however, we also want to keep the coupler relatively narrow to reduce losses (see the end of Sec. I A). The only obvious solution, according to Eq. (20), is to keep the thermoviscous penetration depth δ small compared to the radius r_c of the coupler—in other words, use a high-Q coupler. This suggests that if the working fluid and its ambient state are fixed, the best strategy is to increase all the diameters, thus enabling A_0/A_c to be large while keeping r_c/δ small.

To complement the preceding discussion of how to optimize the coupling, we consider briefly the question of when Eq. (20) is a valid approximation. Equation (20) was derived assuming weak coupling between the resonators; it is fair to suppose that if r_c/δ is big enough, i.e., if the coupler has a high enough Q, then the coupling is not weak. Another way of looking at it, of course, is that the larger the system, or the thinner the boundary layer in the working fluid, the more narrow one can afford to make the coupler and still get the same coupling and the same degree of vibration cancellation.

Another important assumption is that the penetration depth δ is small compared to the coupler radius r_c. For our narrowest couplers, δ/r_c is approximately 0.3; thus it is natural to wonder if Eq. (20) still applies. One could carry all computations out to second order; we will not do so here, but we will mention two corrections one might plausibly add. First, the effective cross-sectional area with which the coupler communicates with the resonators is a little less than πr_c^2, because some of the fluid is viscously clamped at the coupler walls. Thus we might suppose that A_c in Eq. (20) should be replaced by some reduced area A_c', where[18]

$$A_c'\approx\pi r_c^2\left(1-\frac{\delta_\nu}{r_c}\right). \tag{21}$$

Second, a similar correction applies to the length l_c. Since the coupler is narrow and lossy, its effective speed of sound is slower than in the resonators; thus the length that makes the coupler resonant is shorter than l_0, and changes with its radius. Recall that requiring that the coupler be in a half-wavelength resonance is equivalent to making the real part of $\tilde{k}_c l_c$ equal to π; an approximate result for l_c is

$$l_c(\text{resonant})\approx\frac{\pi a_c}{\omega}\left(1-\frac{\delta}{2r_c}\right). \tag{22}$$

Had we not assumed $l_c=l_0$ in the derivation of Eq. (20), the factor $l_c A_0/l_0 A_c$ would have appeared in the result instead of A_0/A_c, so the two corrections above nearly cancel one another. We might expect, then, that Eq. (20) is reasonably accurate even for very narrow couplers.

It is also worth noting that Eq. (20) is independent of any characteristics of the mechanism driving the resonators. Thus Eq. (20) should apply equally well to organ pipes or thermoacoustic engines, when they are acoustically coupled by a resonant tube. However, this is generally *not* true for other (e.g., reactive) types of coupling, such as ''mass coupling'' through the shared structure.

In the following sections, we describe experiments that measure $\partial\phi/\partial\Delta\omega$ for a variety of coupler diameters, and a computer model that simulates these experiments. Both experiment and simulation agree well with the predictions of Eq. (20). Experiments and simulations are also presented for

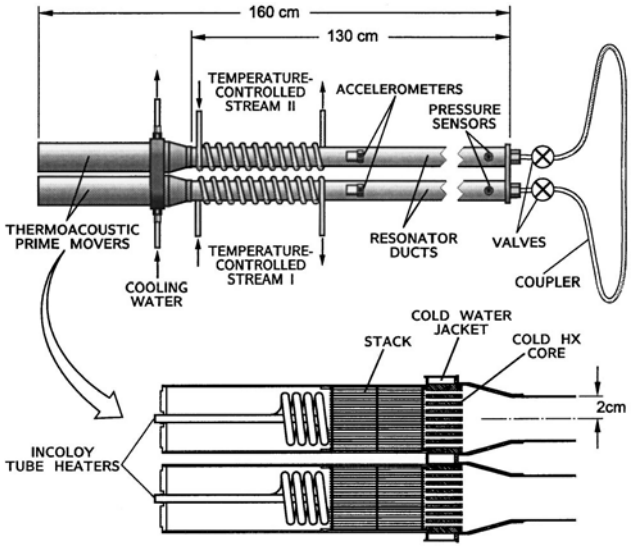

FIG. 4. Experimental setup for exploring the behavior of coupled thermoacoustic engines.

coupled engines whose resonators are not uniform-diameter ducts, in which case Eq. (20) is not quantitatively applicable.

II. APPARATUS

To explore mode-locking of acoustic engines experimentally, we have built two nearly identical thermoacoustic engines which are rigidly attached to each other in a side-by-side fashion. Two neighboring ends of the engines are connected by a coupling duct which can be inserted or removed from the system by means of valves. These are ''straight pattern'' ball valves, which look like a section of straight duct when open, the fluid not following any kind of tortuous path. Each engine consists of a straight, circular duct of uniform diameter (the resonator) connected to a thermoacoustic prime mover, by which we mean a heater, a cold heat exchanger, and a stack of parallel plates in between; these sustain the oscillations in the resonator when the engine is running.

Figure 4 shows the essentials of the experimental setup, and some details of the thermoacoustic prime mover hardware. Note that the engines share a water jacket that cools their cold heat exchangers, and both are welded to a common plate at the other end. A section of each resonator is wrapped with copper refrigeration tubing, which circulates water from a temperature-controlled bath. Thus the gas temperature in each engine can be varied independently, enabling control of $\Delta\omega$, the difference in natural frequencies. A pressure sensor is mounted at the end of each resonator where it joins the coupler. We take the signal from the sensor in resonator I (pressure sensor I) to represent $p_{\mathrm{I}}(t)$, and that from pressure sensor II to represent $p_{\mathrm{II}}(t)$. Using p_{I} as a reference to a lock-in amplifier, and using p_{II} as the input signal, allows a direct measurement of ϕ. Independent monitoring of pressure sensors I and II allows one to obtain $P_{\mathrm{I}}(t)$ and $P_{\mathrm{II}}(t)$. Accelerometers on the cases measure case vibration in the axial (x) direction, and numerous thermocouples (not pictured) provide data on the temperature of the gas near the hot end of the stack, the cooling water temperature, the water jacket temperatures, and the temperature of the gas inside the resonators. Multimeters monitor the input voltage and current to the tube heaters that power the engines. The accelerometers are used to verify that the two engines welded together act like a rigid structure, and that vibrations are indeed canceled when the phase between the engines approaches π—we find that cancellation of case vibration is at least 99.5% complete when $\phi=\pi\pm0.002$.

In order to confirm our analytic and experimental results, we have simulated our system using DELTAE[19] (Design Environment for Low-amplitude ThermoAcoustic Engines). DELTAE integrates the one-dimensional wave equation in the small-amplitude (''acoustic'') approximation, including thermal and viscous effects, according to the thermoacoustic theory of Rott.[20] In our numerical model, we have four geometrically identical engines, two coupled by a narrow duct (which share a common frequency of operation) and two running independently; the gas temperatures in the resonator portion of each of the two coupled engines are varied in order to vary $\Delta\omega$, and the ϕ and ζ values that solve the wave equation in this system are returned by DELTAE. The actual $\Delta\omega$ that exists between the simulated coupled engines is estimated by forcing each uncoupled engine in the model to have the same temperature distribution as one of the coupled engines. For the coupled engines, the input heater power is assumed to be the same in both; however, in order to match gas temperatures at both ends of the stack, the uncoupled engines must use the input heater power as a ''guess'' which can be adjusted to meet the ''targets'' (which include the gas temperatures at the ends of the stack).

Measuring the difference in natural frequencies of the engines is subtle, because it cannot be accomplished when the engines are coupled. The most obvious way to measure $\Delta\omega$ is to measure the beat frequency of the engines when the coupler valves are closed, using a dual-channel oscilloscope to observe p_{I} and p_{II} and timing the beats with a stopwatch. Since $\Delta\omega=\partial\phi/\partial t$ when the engines are uncoupled, where $\partial\phi/\partial t$ is in radians per second, a quick and accurate measurement of $\Delta\omega$ is obtained. Unfortunately, the ''natural frequency'' of an engine is dominated by its mean temperature $T_m(x)$; the temperature at the ''hot end'' of the engine (T_H), in turn, depends on the impedance the prime mover sees looking into the resonator, which depends on whether the coupler valves are open or closed. For instance, assume the input power to an electric heater as shown in Fig. 4 is constant; if the coupler valve, initially closed, is then opened, the load on the engine is increased, causing the pressure amplitude to drop and T_H to rise.[21] Likewise, if the valve is suddenly closed, T_H will begin to fall. The ''natural frequency'' we are trying to measure is, of course, the frequency the engine *would* have with the coupler valves closed, but with the *same* temperature distribution $T_m(x)$ it has in the locked state with the coupler valves open. When we attempt to measure the $\Delta\omega$ corresponding to a given locked state by opening the coupler valves and observing $\partial\phi/\partial t$, we are actually looking at the engines in an ambiguous state where their temperatures, and hence their frequencies, are changing with time.

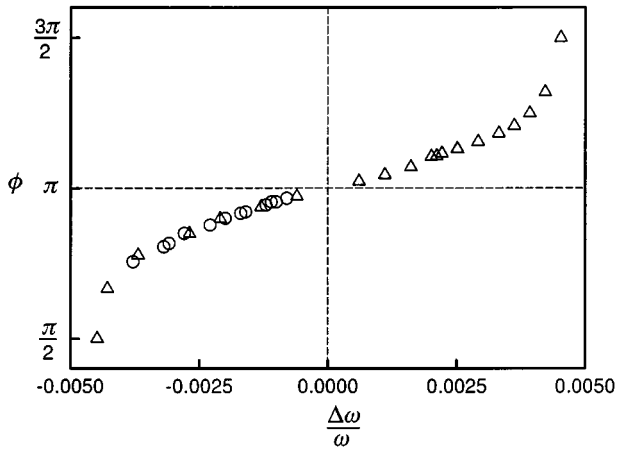

FIG. 5. Relative phase ϕ versus fractional mistuning $\Delta\omega/\omega$ for two acoustically coupled thermoacoustic engines. For the circular data points, the engines were allowed to thermally equilibrate with the coupling valves open; for the triangular points, the engines equilibrated with the coupling valves closed.

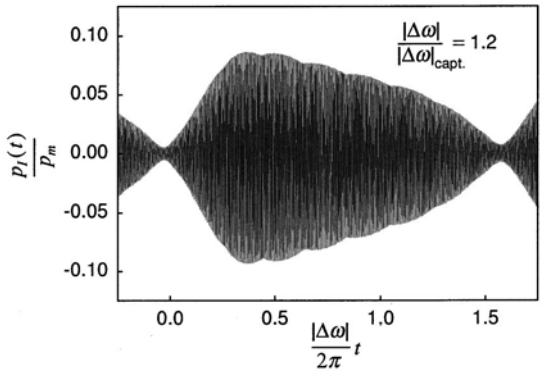

FIG. 6. Oscillating pressure versus time for one of two coupled thermoacoustic engines, when their frequency mismatch $\Delta\omega$ is 20% larger than the capture bandwidth. The oscillating pressure $p_1(t)$ is normalized to the mean pressure p_m, and the time t is normalized to the beat period in the absence of coupling, $2\pi/\Delta\omega$, thus showing the period elongation. (The slight rippling of the beat envelope is due to aliasing.)

In this work, we employ two basic strategies for resolving this ambiguity:

(1) Measure $\phi(\Delta\omega)$ two ways:
   (a) Let engines equilibrate with coupler valves open; measure ϕ. Close valves and immediately measure $\Delta\omega$.
   (b) Let engines equilibrate with coupler valves closed; measure $\Delta\omega$. Open valves and immediately measure ϕ. Compare with (a).
(2) In computer model, force $T_m(x)$ in each engine to be the same in both coupled and uncoupled states; compare simulation results for $\phi(\Delta\omega)$ with 1(a) and 1(b).

We find that for the purposes of the present work, the difference between the results obtained by 1(a) and 1(b) is small; since we are interested in characterizing the locked state of the engines, method 1(a) is used for all the data presented in this paper, unless otherwise specified.

Changes in T_H with load do not interfere too much with the measurement of $\Delta\omega$ for two reasons: $\Delta\omega$ is dominated by the difference in resonator gas temperature, which is set by the separate temperature control coils; and the engines never have a large amplitude difference with a resonant coupler, so any change in T_H with load tends to be the same in both engines. These conditions do not necessarily exist for other types of coupling, such mass coupling.

III. RESULTS

Figure 5 shows typical behavior of the phase ϕ between the engines in the locked state versus the fractional mistuning $\Delta\omega/\omega$, for the system shown in Fig. 4. The coupler has about a 3-mm inner diameter; the working fluid is air at 0.8 bar, and the frequency of operation is about 100 Hz. The circles are data points taken according to method 1(a) mentioned in the previous section, where the engines equilibrate with the coupler valves open; the triangles are data points taken using method 1(b), where the engines equilibrate with the valves closed. Apparently the two methods agree well.

Figure 5 displays a *capture bandwidth* of $(|\Delta\omega|/\omega)_{\text{capt.}} \approx 0.004$, or 0.4%, with band-edges near $\phi = \pi \pm \pi/2$, where the capture bandwidth is defined as the maximum natural frequency difference the engines can have and still achieve locking. It is apparent that $\phi(\Delta\omega)$ has a linear region near $\phi = \pi$; this is where we expect Eq. (20) to apply. Nearer the capture band-edge, ϕ changes very rapidly with $\Delta\omega$, until the engines unlock at $\phi = \pi \pm \pi/2$. The data points shown at $\phi = \pi \pm \pi/2$ are not in fact true, stable locked states; the phase tends to oscillate with a period of about a minute with an amplitude of $\pi/10$ or more. These states are hysteretic, in that locking initially occurs only for $0.7\pi < \phi < 1.3\pi$, but after locking is achieved, it will hold for phase angles closer to the band-edge. Just beyond the band-edge, the engines are unlocked and beat against each other; unlike a linear system, the beat frequency is slower than $\Delta\omega$ and the beat envelope is not sinusoidal. These features are evident in Fig. 6, which shows one beat cycle of the pressure p_1 when the engines have been detuned 20% beyond the capture bandwidth.

One other feature of Fig. 5 worth noting is the gap in the data near $\phi = \pi$, the region of most interest to us. When $\Delta\omega$ is sufficiently small, the ability of the engines to exert forces on each other through their shared structure, what we have called the ''mass coupling,'' is sufficient to elongate the beat period or even cause mode-locking; thus it is impossible to get an accurate estimate of $\Delta\omega$ by the methods mentioned previously, since the engines cannot be considered uncoupled when the coupler valves are closed. We detail mass coupling phenomena in a separate paper;[8] here we simply note that the capture bandwidth for mass coupling depends on how massive the case is compared to the gas inside, the bandwidth being larger when the case is relatively light. In the present work, therefore, we eliminate the mass coupling in subsequent data sets by attaching additional mass to our twin-engine assembly (we add an extra 130 kg of mass, which increases the system's solid mass by more than a factor of 10).

Figure 7 shows $\phi - \pi$ and $\zeta - 1$ for our mode-locked engines near $\phi = \pi$; the working fluid is air at 0.8 bar and 300 K, and the coupler is 3.2 mm in diameter and its length

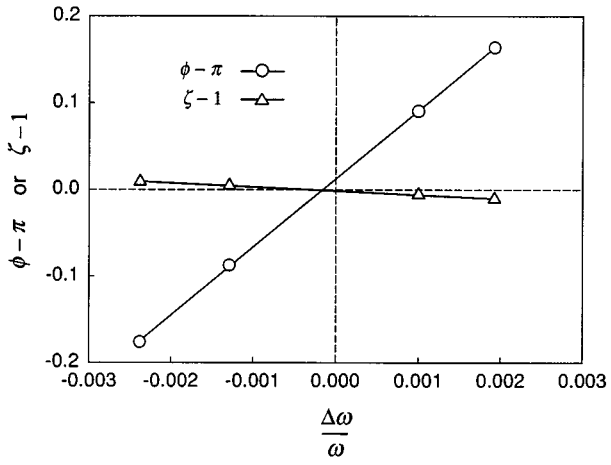

FIG. 7. Plots of $\phi-\pi$ and $\zeta-1$ vs $\Delta\omega/\omega$ for system of Fig. 4, where working fluid is air at 0.8 bar and 300 K; coupler has a diameter of 3.2 mm, and its length is chosen to make it resonant. Note that $\phi-\pi$ and $\zeta-1$ are plotted to the same scale.

is chosen to make it resonant. Recall from Eq. (6) that the cancellation ratio $R_V \approx 1-[(\phi-\pi)^2+(\zeta-1)^2]^{1/2}$; with the resonant coupler in place, it is apparent that the case vibration is dominated by the phase angle ϕ, the amplitude mismatch $\zeta-1$ being relatively negligible, as predicted by theory. Additional measurements verify that if the coupler length l_c is made even a few percent larger or smaller than the resonant length $(\pi a_c/\omega)(1-\delta/2r_c)$, $\zeta-1$ increases dramatically.

The main objective of our experiments is to measure $\partial\phi/\partial\Delta\omega$ as a function of coupling strength, which we vary by changing coupler diameter. Data of the type in Fig. 7 were recorded with air at 0.8 bar, 300 K as the working fluid, for couplers of five different diameters, ranging from 2.7 mm ($A_0/A_c=185$, $\delta/r_c=0.29$) to 4.8 mm ($A_0/A_c=58$, $\delta/r_c=0.16$). In all cases, the resonator radius r_0 remains constant at 1.82 cm, and the coupler length l_c is chosen to make the coupler resonant. The results are summarized in Fig. 8, in which each data point represents the slope of a data set like that of Fig. 7, scaled by $1/\pi$. It is evident that experiment, theory, and simulation are all in excellent agreement, implying that the mode-locking of uniform diameter, circular duct resonators coupled by a resonant, half-wavelength duct is

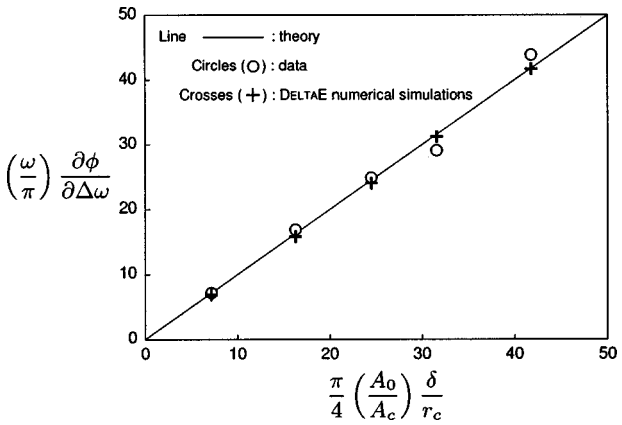

FIG. 8. Summary of $\partial\phi/\partial\Delta\omega$ results for thermoacoustic engines coupled by resonant half-wavelength ducts of various diameters.

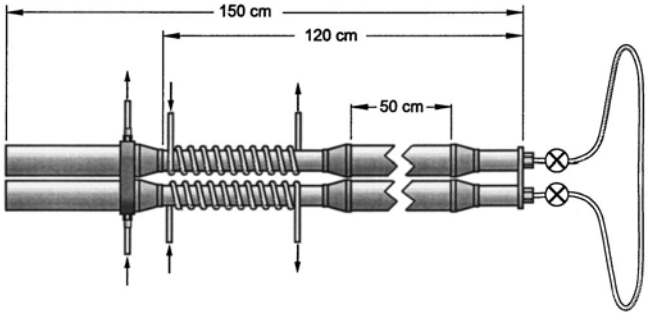

FIG. 9. Engines used for the measurements in Sec. III; these use the same prime movers as the first set of measurements, but the resonator shape has been altered to suppress distortion at high amplitudes.

well understood to first order. The disagreements between experiment and theory are on the order of a few percent, which is about the precision to which the inner radii of the couplers are determined.

Engine resonators are not necessarily cylindrical ducts of uniform cross section, as was assumed when deriving Eq. (20) and other formulas. A resonator with varying cross section may be shorter than a uniform duct of the same natural frequency, it may suppress harmonic generation at high amplitudes, and it may decrease dissipation at low amplitudes. Rather than present a theory[8] for arbitrary resonator shape, we consider one limiting case, to gain insight, and compare its predictions with experiments and simulations.

We consider the limiting case of two coupled Helmholtz resonators, each consisting of two volumes V_1 and V_2 connected by a duct area A_0 and length l. The two V_2's are connected by a coupling duct of radius r_c and length $l_c \sim \lambda/2$. We find that

$$\left(\frac{\omega}{\pi}\right)\frac{\partial\phi}{\partial\Delta\omega} \simeq \frac{\pi}{4}\left(\frac{A_0}{A_c}\right)\frac{\delta}{r_c}\left[4\,\frac{V_1+V_2}{\lambda A_0}\left(\frac{V_2}{V_1}\right)\right] = \frac{\pi}{4}\left(\frac{A_0}{A_c}\right)\frac{\delta}{r_c}F_H, \tag{23}$$

where F_H is what we call the ''Helmholtz factor.'' This formula reverts to Eq. (20), the half-wave resonator result, if $V_1=V_2=V=A_0(\lambda/8)$, and if $l=(4/\pi^2)\lambda$ (which forces the Helmholtz resonator frequency to be the same as the half-wave resonator). Together, l and V describe a plausible mass-spring model of a half-wave resonator. This says the ''effective mass,'' in this context, of the oscillating fluid in a half-wave resonator is about 0.8 of its total mass.

Most importantly, we note that $\partial\phi/\partial\Delta\omega$ has the same dependence on r_c and δ for coupled Helmholtz resonators as for half-wave ducts. This suggests that any data on resonators of arbitrary shape should still lie on a straight line on a graph such as Fig. 8, but with a slope that may differ from unity.

Experiments were done using a setup identical to that shown in Fig. 4, except the resonators were altered as shown in Fig. 9, with a shorter overall length and a sizable section of duct near the coupled ends that is about twice the cross-sectional area of the original duct. This particular design was chosen to make the first and second overtones of the resona-

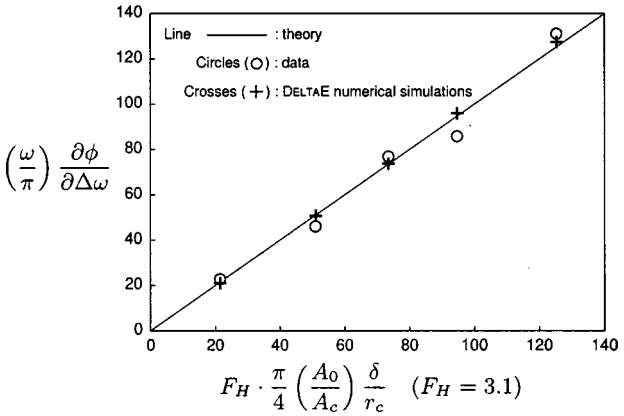

FIG. 10. Summary of $\partial\phi/\partial\Delta\omega$ results for thermoacoustic engines coupled by resonant half-wavelength ducts of various diameters, with the engine resonators having the shape pictured in Fig. 9.

tor lie half-way between harmonics of the fundamental, to suppress distortion at high amplitudes, while keeping the fundamental frequency the same as before. Data of the type shown in Fig. 7 were taken for the same five couplers; the $\partial\phi/\partial\Delta\omega$ results, along with DELTAE simulations of this system, are summarized in Fig. 10. The abscissa has one adjustable parameter, F_H [as defined in Eq. (23)], which is chosen to best fit the data. With F_H properly adjusted, experiment, theory and simulation are in excellent agreement. The general theory for arbitrarily shaped resonators has been derived by us.[8] These results, and those in the previous section, give us confidence that DELTAE can be relied upon to help design systems more complex than those we can readily analyze.

IV. APPLICATION TO VIBRATION CANCELLATION

The application of the results in the previous section to the vibration cancellation problem is straightforward. Typically, one might desire a given level of vibration cancellation, with two engines that are likely to experience a known (or estimated) range of detuning, and one would like to know what length and radius coupler is necessary to achieve the desired cancellation. In other words, given a desired R_V as in Eq. (6), and an expected $|\Delta\omega|$, we want to find l_c and r_c. We assume that the working fluid and its state are fixed; thus δ is known. If we assume a resonant coupler, then $|\phi-\pi| \gg |\zeta - 1|$, and $R_V \approx 1-|\phi-\pi|$. Then the slope of $\phi(\Delta\omega)$ at zero is related to the desired vibration cancellation and the maximum estimated $|\Delta\omega/\omega|$ by

$$\frac{1-R_V(\text{desired})}{|\Delta\omega/\omega|(\text{max, est})} = \omega\frac{\partial\phi}{\partial\Delta\omega} = \frac{\pi^2}{4}\left(\frac{\pi r_0^2}{\pi r_c^2}\right)\frac{\delta}{r_c}F_H. \quad (24)$$

This can be solved for r_c to yield

$$r_c = \left[\frac{\pi^2}{4}r_0^2\delta\frac{|\Delta\omega/\omega|}{1-R_V}F_H\right]^{1/3}; \quad (25)$$

the resulting value for r_c can be substituted along with δ into Eq. (22) to obtain l_c.

Suppose, for instance, that we have two engines using helium gas at 30 bar, 300 K, and whose resonators have a radius of 15 cm, with $F_H=1$ (e.g., resonators of uniform diameter). Suppose they may vary as much as 1% in natural frequency during operation, and we want to eliminate 95% of the vibration. Thus we have $\delta=0.3$ mm, $r_0=15$ cm, $|\Delta\omega/\omega|=0.01$, and $R_V=0.95$. According to Eq. (25), the minimum coupler radius is $r_c\approx 1.5$ cm.

An additional constraint one is likely to face is the maximum additional dissipation, due to the coupler, that can be tolerated. According to the simple ideas at the end of Sec. I A, the dissipation in the coupler is simply (r_c/r_0) times the dissipation in a main resonator.[22] This is only strictly true at $\phi=\pi$, where the pressure and velocity profiles in the coupler are the same as in the resonators. When $\phi\neq\pi$, the asymmetry in the boundary conditions of the coupler causes its pressure and velocity amplitudes to increase; this can be seen by looking at Eq. (13). Let the thermoviscous dissipation in a resonator be $\dot{E}_0$, and that in the coupler be $\dot{E}_c$. If we assume a resonant coupler, and $\phi\approx\pi$, hence $\zeta=1$, we find that

$$\frac{\dot{E}_c}{\dot{E}_0} \approx \frac{r_c}{r_0}\left[1+\left(\frac{|\phi-\pi|}{\pi}\frac{r_c}{\delta/2}\right)^2\right]; \quad (26)$$

we can use Eq. (23), the relationship between $|\phi-\pi|$ and $\Delta\omega$, to rewrite this as:

$$\frac{\dot{E}_c}{\dot{E}_0} \approx \frac{r_c}{r_0}\left[1+\frac{\pi^2}{4}F_H\left(\frac{\Delta\omega}{\omega}\right)^2\left(\frac{r_0}{r_c}\right)^4\right]. \quad (27)$$

For a given $\Delta\omega/\omega$, there will exist an optimum r_c/r_0 for which the dissipation in the coupler is a minimum; it is found to be

$$\left.\frac{r_c}{r_0}\right|_{\text{opt.}} \approx \left[\frac{3\pi^2}{4}F_H\left(\frac{\Delta\omega}{\omega}\right)^2\right]^{1/4}. \quad (28)$$

For the large-diameter system considered above, where the maximum $|\Delta\omega/\omega|=1\%$, this formula predicts $(r_c/r_0)_{\text{opt.}} = 1/6$ [DELTAE predicts $(r_c/r_0)_{\text{opt.}}=0.17$]; if $r_0=15$ cm, this implies $r_c=2.5$ cm, about 5/3 times the minimum radius needed to achieve the desired vibration cancellation. In other words, because of the increased dissipation that occurs with increasing $\Delta\phi$, one gets less dissipation overall by using a larger-diameter coupler and keeping $\Delta\phi$ small, even though this increases the surface area of the coupler. In this example, the 2.5-cm-radius coupler dissipation is about 15% of resonator dissipation when $|\Delta\omega/\omega|=0$, and increases to a little over 20% when $|\Delta\omega/\omega|=0.01$. On the other hand, the 1.5-cm-radius coupler dissipation is only 10% of resonator dissipation at $|\Delta\omega/\omega|=0$, but rises to over 30% when $|\Delta\omega/\omega|=0.01$.

Thus in choosing the proper coupler radius, one must consider not only how much vibration or dissipation can be tolerated, but also how often and for how long the engines might be expected to operate in the extremes of the expected range of detuning. It may be better to use the minimum r_c specified by Eq. (25), or an even narrower one, if the engines will only rarely experience significant detuning. Equations such as Eq. (23), Eq. (25), and Eq. (28) are but helpful guides in making an intelligent choice.

The above results apply in the low-amplitude limit, where turbulence is unimportant. To achieve a useful power density, a practical device may need to operate at a high amplitude. In the limit of very high Reynolds number, where the Moody friction factor[23] becomes nearly constant with amplitude, we estimate that the same optimum ratio (r_c/r_0) as before will give the minimum dissipation. A more complicated, but not implausible, scenario is one where the narrow coupler has a much higher peak Moody friction factor than the resonator, in which case high velocities in the coupler could be very costly. Widening the coupler would not only reduce $\Delta\phi$, reducing the peak velocity in the coupler, but also reduce its friction factor. Thus the amplitude at which the engines operate is another consideration in optimizing the coupling.

This work is exclusively devoted to couplers which are circular ducts of constant cross-section, of nominal length $\lambda/2$. One may wonder if other coupler shapes might provide the same degree of coupling, with fewer losses. We have little experimental data on alternate coupler shapes, but in our computer simulations, we have explored many different coupler shapes and designs, as well as placement of the coupler at points on the resonator other than the pressure antinodes. We have never found a design that gives as much coupling for as little loss as a uniform-diameter circular duct. It is often advantageous to ''neck down'' a portion of a resonator, because compared to a uniform-diameter duct at the same frequency, it reduces the surface area for dissipation more than it increases the particle velocity, resulting in less dissipation overall.[24] For a coupler, however, necking down the duct decreases the coupling strength; this and other factors make it appear that the uniform-diameter coupler is optimum.

ACKNOWLEDGMENTS

The authors wish to thank Bob Keolian and Bob Ecke for teaching us about mode-locking, Bill Ward, Scott Backhaus, and Bob Hiller for useful discussions, and David Gardner for assistance with the experiments. This work has been supported by the offices of Fossil Energy and Basic Energy Sciences in the U.S. Department of Energy.

[1] G. W. Swift, ''Thermoacoustic engines and refrigerators,'' Phys. Today **48**, 22–28 (July 1995); S. Backhaus and G. W. Swift, ''A thermoacoustic Stirling heat engine,'' Nature **399**, 335–338 (1999).

[2] C. Sondhauss, ''Ueber die schallschwingungen der luft in erhitzten glasröhren und in gedeckten pfeifen von ungleicher weite,'' Ann. Phys. (Leipzig) **79**, 1 (1850).

[3] ''A simple theory of the Sondhauss tube,'' in *Recent Advances in Aeroacoustics*, edited by A. Krothapalli and C. A. Smith (Springer, New York, 1984), p. 327.

[4] P. L. Rijke, ''Notiz über eine neue art, die in einer an beiden enden offenen röhre enthaltene luft in schwingungen zu versetzen,'' Ann. Phys. (Leipzig) **107**, 339 (1859).

[5] G. W. Swift, ''Thermoacoustic natural gas liquefier,'' 1997, in Proceedings of the DOE Natural Gas Conference, Houston TX, March 1997.

[6] W. A. Marrison, U.S. Patent No. 2,836,033 (1958).

[7] C. Huygens, in *Ouevres Completes de Christian Huyghens*, edited by M. Nijhoff, Vol. 5, p. 243 (Societe Hollandaise des Sciences, The Hague, The Netherlands, 1893) (A letter to his father, dated 26 Feb. 1665).

[8] P. S. Spoor and G. W. Swift, ''The Huygens phenomenon in thermoacoustics,'' in preparation for J. Acoust. Soc. Am.

[9] In Ref. 8, we find that mass coupling obeys $\partial\phi/\partial\Delta\omega = 1/(\omega Q\mu^2)$, where μ is the ratio of working fluid mass to case mass $(m_{\rm gas}/m_{\rm case})$. For the realistic, large-diameter system (Ref. 5) discussed in Sec. IV in the text, comparing this result with Eq. (20) shows that the acoustic coupling is of order 10 000 times stronger than the mass coupling.

[10] A. B. Pippard, *The Physics of Vibration* (*Omnibus Edition*) (Cambridge University Press, Cambridge, 1989), Chap. 12.

[11] Reference 10, p. 403.

[12] Reference 10, p. 323.

[13] B. Van der Pol, ''The nonlinear theory of electric oscillations,'' Proc. Inst. Rad. Eng. **22**, 1051 (1934).

[14] The value of n can be determined either from the relaxation time of the oscillator from one amplitude to another, or from changes in steady-state amplitude in response to changes in load. For our thermoacoustic engines, only the steady state is well characterized, for when the engine is relaxing from one state to another, the power input is ambiguous, the thermal mass of the engine absorbing or supplying heat at a variable rate. Changes in steady state amplitude only determine the quantity n/Q, and cannot obtain n or Q independently. Fortunately, for the purposes of this work and that in Ref. 8, this is sufficient.

[15] P. M. Morse, *Vibration and Sound* (American Institute of Physics, Woodbury, NY, 1986), p. 313.

[16] S. Backhaus, ''Search for acoustic Josephson radiation in superfluid ^{4}He,'' Ph.D. thesis, University of California at Berkeley, 1997.

[17] N. H. Fletcher, ''Mode-locking in nonlinearly excited inharmonic musical oscillators,'' J. Acoust. Soc. Am. **64**, 1566 (1978). See also the URL www.csu.edu.au/ci/vol1/Neville.Fletcher/.

[18] A. M. Fusco, W. C. Ward, and G. W. Swift, ''Two-sensor power measurements in lossy ducts,'' J. Acoust. Soc. Am. **91**, 2229–2235 (1992).

[19] W. C. Ward and G. W. Swift, ''Design environment for low amplitude thermoacoustic engines (DELTAE),'' J. Acoust. Soc. Am. **95**, 3671–3672 (1994). Fully tested software and user's guide available from Energy Science and Technology Software Center, US Department of Energy, Oak Ridge, Tennessee. To review DeltaE's capabilities, visit the Los Alamos thermoacoustics web site at www.lanl.gov/thermoacoustics/. For a beta-test version, contact ww@lanl.gov (Bill Ward) via Internet.

[20] N. Rott, ''Thermoacoustics,'' Adv. Appl. Mech. **20**, 135–175 (1980).

[21] J. R. Olson and G. W. Swift, ''A loaded thermoacoustic engine,'' J. Acoust. Soc. Am. **98**, 2690–2693 (1995).

[22] The ratio of coupler to resonator dissipation, even at $\phi = \pi$, is generally a little higher than r_c/r_0, because the engines never have a completely uniform cross-section, which makes them shorter for a given frequency, thus lessening their surface areas. In Fig. 4, the hot ends of the engines are wider than the resonators, to provide more power, and the length of the engines is hence shortened to 0.44λ.

[23] L. F. Moody, ''Friction factors for pipe flow,'' Trans. ASME **66**, 671–684 (1944).

[24] T. J. Hofler, ''Thermoacoustic refrigerator design and performance,'' Ph.D. thesis, Physics department, University of California, San Diego, 1986.